

Strong-field quantum control by pulse shaping in the extreme ultraviolet domain

Fabian Richter¹, Ulf Saalmann², Enrico Allaria³, Matthias Wollenhaupt⁴, Benedetto Ardingi⁵, Alexander Brynes³, Carlo Callegari³, Giulio Cerullo⁵, Miltcho Danailov³, Alexander Demidovich³, Katrin Dulitz⁶, Raimund Feifel⁷, Michele Di Fraia^{3,8}, Sarang Dev Ganeshamandiram¹, Luca Giannessi^{3,9}, Nicolai Gözl¹, Sebastian Hartweg¹, Bernd von Issendorff¹, Tim Laarmann^{10,11}, Friedemann Landmesser¹, Yilin Li¹, Michele Manfredda³, Cristian Manzoni¹², Moritz Michelbach¹, Arne Morlok¹, Marcel Mudrich¹³, Aaron Ngai¹, Ivaylo Nikolov³, Nitish Pal³, Fabian Pannek¹⁴, Giuseppe Penco³, Oksana Plekan³, Kevin C. Prince³, Giuseppe Sansone¹, Alberto Simoncig³, Frank Stienkemeier¹, Richard James Squibb⁷, Peter Susnjar³, Mauro Trovo³, Daniel Uhl¹, Brendan Wouterlood¹, Marco Zangrando^{3,8}, Lukas Bruder^{1,*}

¹Institute of Physics, University of Freiburg, Hermann-Herder-Str. 3, D-79104 Freiburg, Germany

²Max-Planck-Institut für Physik komplexer Systeme, Nöthnitzer Str. 38, 01187 Dresden, Germany

³Eletra-Sincrotrone Trieste S.C.p.A., 34149 Basovizza (Trieste), Italy

⁴Institute of Physics, University of Oldenburg, Carl-von-Ossietzky-Str. 9-11, 26129 Oldenburg, Germany

⁵IFN-CNR, Dipartimento di Fisica, Piazza L. Da Vinci 32, 20133 Milan, Italy

⁶Institut für Ionenphysik und Angewandte Physik, Universität Innsbruck, 6020 Innsbruck, Austria

⁷Department of Physics, University of Gothenburg, Origovägen 6 B, SE-412 96 Gothenburg, Sweden

⁸Istituto Officina dei Materiali - CNR (CNR-IOM), Strada Statale 14 – km 163.5, Trieste, 34149, Italy

⁹Istituto Nazionale di Fisica Nucleare - Laboratori Nazionali di Frascati, Via E. Fermi 40, 00044 Frascati, Roma

¹⁰Deutsches Elektronen-Synchrotron DESY, Notkestr. 85, 22607 Hamburg, Germany

¹¹The Hamburg Centre for Ultrafast Imaging CUI, Luruper Chaussee 149, 22761 Hamburg, Germany

¹²IFN-CNR, Piazza L. Da Vinci 32, 20133 Milan, Italy

¹³Department of Physics and Astronomy, Aarhus University, Ny Munkegade 120, DK-8000 Aarhus, Denmark

¹⁴Institute for Experimental Physics, University of Hamburg, Luruper Chaussee 149, 22761 Hamburg, Germany

Abstract—Tailored light-matter interactions in the strong coupling regime enable the manipulation and control of quantum systems with up to unit efficiency, with applications ranging from quantum information to photochemistry. While strong light-matter interactions are readily induced at the valence electron level using long-wavelength radiation, comparable phenomena have been only recently observed with short wavelengths, accessing highly-excited multi-electron and inner-shell electron states. However, the quantum control of strong-field processes at short wavelengths has not been possible, so far, due to the lack of pulse shaping technologies in the extreme ultraviolet (XUV) and X-ray domain. Here, exploiting pulse shaping of the seeded free-electron laser (FEL) FERMI, we demonstrate the strong-field quantum control of ultrafast Rabi dynamics in helium atoms with high fidelity. Our approach unravels the strong-field induced bound-continuum coupling of the electronic states in helium and enables substantial suppression of the ionization rate, with prospective applications in many XUV and X-ray experiments. Leveraging recent advances in intense few-femtosecond to attosecond XUV to X-ray light sources, our results open an avenue to the efficient manipulation and selective control of core electron processes and electron correlation phenomena in real time.

I. INTRODUCTION

Strong-field phenomena play an important role in our understanding of the quantum world. Light-matter interactions be-

yond the perturbative limit can substantially distort the energy landscape of a quantum system, which forms the basis of many intriguing strong-field effects [1] and opens an avenue for efficient quantum control schemes [2, 3]. Moreover, resonant strong coupling induces rapid Rabi cycling of the level populations [4], enabling complete population transfer to a target state [5]. The development of intense XUV and X-ray light sources [6, 7] has recently permitted the investigation of related phenomena beyond valence electron dynamics, in highly excited, multi-electron and inner-shell electron states [8–14]. Yet in most of these studies, the dressing of the quantum systems was induced by intense infrared fields overlapping with the XUV/X-ray pulses. In contrast, the alteration of energy levels directly by short-wavelength radiation is more difficult. So far, only a few studies reported XUV-induced AC-Stark shifts of moderate magnitude ($\lesssim 100$ meV), difficult to resolve experimentally [14–19].

The active control of quantum dynamics using tailored light fields marks another important quest in exploring and mastering the quantum world [20–22]. At long wavelengths, sophisticated pulse shaping techniques facilitate the precise quantum control and even the adaptive-feedback control of many light-induced processes, both in the weak- and strong-field regime [23–26]. Comparable developments at short wavelengths are hindered by the lack of pulse shaping technologies,

*lukas.bruder@physik.uni-freiburg.de

albeit several studies have pointed out the potential of pulse shaping in XUV and X-ray experiments [27–30]. As a first experimental step in this direction, phase-locked mono- and poly-chromatic pulse sequences have been generated [31–34]. Using this tool, first coherent control demonstrations in the perturbative limit [31, 34, 35] and the generation of intense attosecond pulses were achieved [36, 37]. Moreover, ultrafast polarization shaping at XUV wavelengths was reported recently [38]. However, the feasibility of spectral phase shaping, which forms the core of pulse shaping techniques, has not been demonstrated for the control of quantum phenomena at short wavelengths. Here, we establish spectral phase shaping of intense XUV laser pulses and demonstrate high fidelity quantum control of transiently dressed states in the strong-field limit.

II. RESULTS

In the experiment, He atoms are dressed and ionized by intense coherent XUV pulses delivered by the seeded FEL FERMI (Fig. 1a). Driving the $1s^2 \rightarrow 1s2p$ atomic resonance with a near-resonant intense field $E(t)$ leads to rapid cycling of ground and excited state populations with the generalized Rabi frequency $\Omega = \hbar^{-1} \sqrt{(\mu E)^2 + \delta^2}$, where μ denotes the transition dipole moment of the atomic resonance and δ the energy detuning. A suitable model to describe the non-perturbative quantum dynamics is the dressed-state formalism based on hybrid electron-photon eigenstates [39]. The eigenenergies of the mixed states depend on the field intensity and show the characteristic Autler-Townes (AT) energy splitting $\Delta E = \hbar\Omega$ [40]. The observation of this phenomenon requires the mapping of the transiently dressed level structure while perturbed by the external field [41]. This is achieved by immediate photoionization, projecting the level structure onto the electron kinetic energy (eKE) distribution (Fig. 1b).

Figure 2 demonstrates experimentally the dressing of the He atoms. The build-up of the AT doublet is clearly visible in the raw photoelectron spectra as the XUV intensity increases (Fig. 2a). The evolution of the AT doublet splitting is in good agreement with the expected square-root dependence on the XUV intensity $\Delta E = \mu \sqrt{2I_{\text{eff}}}/(\epsilon_0 c)$. Here, I_{eff} denotes an effective peak intensity, accounting for the spatially averaged intensity distribution in the interaction volume, ϵ_0 , c denote the vacuum permittivity and the speed of light, respectively. The data can be thus used for gauging the XUV intensity in the interaction volume, a parameter otherwise difficult to determine. At the maximum XUV intensity, the photoelectron spectrum shows an energy splitting exceeding 1 eV, indicative of substantial AC-Stark shifts in the atomic level structure. The large AT splitting further implies that a Rabi flopping within 2 fs is achieved, offering a perspective for rapid population transfer outpacing possible competing intra and inter atomic decay mechanisms, which are ubiquitous in XUV and X-ray applications [42].

Figures 2b,c show the photoelectron yield as a function of excitation photon energy. For high XUV intensity (Fig. 2b), the photoelectron spectra reveal an avoided level crossing of the dressed He states as they are mapped to the electron

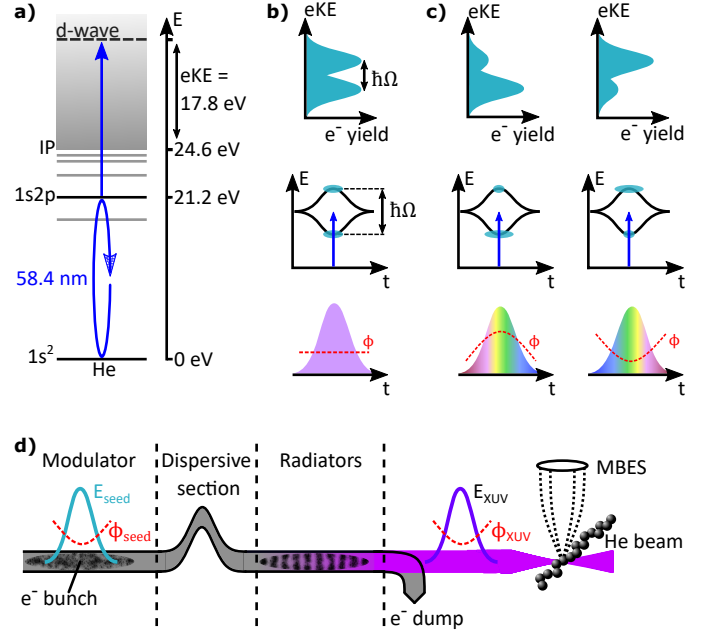


Figure 1. XUV strong-field coherent control scheme in He. (a) Intense XUV pulses induce Rabi-cycling in the He $1s^2 \rightarrow 1s2p$ resonance and photoionize the atoms to map the Rabi dynamics to the electron continuum. (b,c) The strong driving of the atomic system induces a transient AT splitting in the dressed energy levels (middle panel). The ultrafast temporal evolution of the AT doublets follows the intensity profile of the XUV field (lower panel). The dressed-state populations are monitored in the photoelectron eKE distributions (upper panel). XUV pulse shaping enables the control of the non-perturbative quantum dynamics. For a flat phase ϕ , both excited dressed states are equally populated. For a positive phase curvature the population is predominantly transferred to the lower dressed state and the upper state is depleted, while for negative curvature the situation is reversed. (d) Principle of XUV pulse shaping at the FEL FERMI. Intense seed laser pulses overlap spatially and temporally with the relativistic electron bunch in the modulator section of the FEL, leading to a modulation in the electron phase space. The induced energy modulations are converted into electron-density oscillations upon passing a dispersive magnet section. The micro-bunched electrons then propagate through a section of radiator undulators, producing a coherent XUV pulse. In this process the phase function of the seed pulse is coherently transferred to the XUV pulse, resulting in precise XUV phase shaping. The FEL pulses are focused into the interaction volume, exciting and ionizing He atoms. The photoelectrons are detected with a magnetic bottle electron spectrometer (MBES).

continuum (see also Fig. 4). Accordingly, at lower XUV intensity (Fig. 2c), the avoided crossing is not visible anymore. In the latter, the eKE distribution centers at 17.9 eV. At the same kinetic energy, a similar contribution overlays the photoelectrons emitted from the strongly dressed atoms in Fig. 2b. Likewise, a significant portion of photoelectrons at $eKE \approx 17.9$ eV in Fig. 2a does not show a discernible AT splitting. We conclude that a fraction of He atoms in the ionization volume are excited by much lower FEL intensity, which is consistent with the aberrated intensity profile of the FEL measured in the ionization volume (Supp. Info. I). This overlapping lower intensity contribution does not influence the interpretation of the results in this work. For better visibility of the main features, we thus subtract this contribution from the data shown in Fig. 3 and 4.

The demonstrated dressing of He atoms provides one prerequisite for implementing quantum control of non-perturbative dynamics in the XUV domain. The second crucial

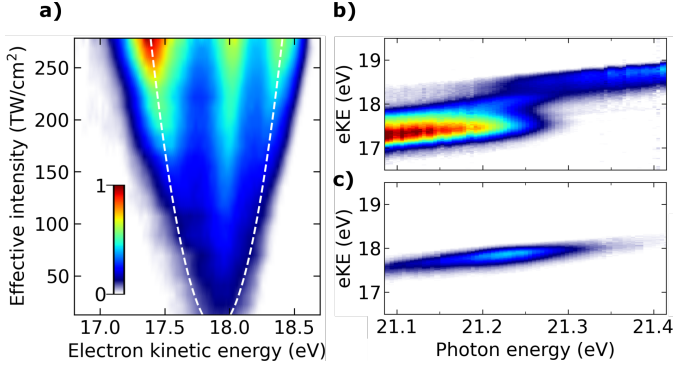


Figure 2. Build-up of the Autler-Townes splitting in He atoms. (a) Detected photoelectron eKE distribution (raw data) as a function of the XUV intensity (FEL photon energy: 21.26 eV). Dashed lines show the calculated AT splitting for an effective XUV peak intensity I_{eff} accounting for the spatial averaging in the interaction volume (values given on y-axis). (b) Photoelectron spectra as a function of photon energy recorded for high XUV intensity ($I_{\text{eff}} = 2.92(18) \times 10^{14} \text{ W/cm}^2$) and in (c) for lower intensity ($I_{\text{eff}} \approx 10^{13} \text{ W/cm}^2$). In (b), a clear avoided crossing between the lower/higher AT band is visible directly in the raw photoelectron spectra. The photoelectron distribution peaking at eKE=17.9 eV in (a) and (b) is ascribed to He atoms excited by lower XUV intensity (see text).

ingredient is the ability to shape the phase of the XUV field. The physical mechanism underlying the control scheme is described in the framework of the selective population of dressed states (SPODS) [43], illustrated in Fig. 1b,c. A flat phase leads to an equal population of both dressed states in the excited state manifold, whereas a positive/negative phase curvature results in a predominant population of the lower/upper dressed state, respectively (Fig. 1c). The scheme has been experimentally demonstrated with long-wavelength radiation [44], where pulse shaping techniques are readily available. However, the opportunities of pulse shaping technologies are largely unexplored for XUV and X-ray radiation.

We solve this problem by exploiting the potential of seeded FELs to allow for the accurate control of XUV pulse properties [45–47]. The seeded FEL FERMI operation is based on the high-gain harmonic generation (HGHG) principle [48], where the phase of an intense seed laser pulse is imprinted into a relativistic electron pulse to precondition the coherent XUV emission at harmonics of the seed laser (Fig. 1d). For FEL operation in the linear amplification regime, the phase $\phi_{nH}(t)$ of the FEL pulses emitted at the n 'th harmonic of the seed laser follows the relationship [45]

$$\phi_{nH}(t) \approx n[\phi_s(t) + \phi_e(t)] + \phi_a. \quad (1)$$

Here, ϕ_s denotes the phase of the seed laser pulses, which can be tuned with standard pulse shaping technology at long wavelengths (see Methods for details). ϕ_e accounts for the possible phase shifts caused by the energy dispersion of the electron beam through the dispersive magnet and is negligible for the parameters used in the experiment. ϕ_a accounts for the FEL phase distortion due to the amplification and saturation in the radiator and has been kept negligibly small by properly tuning the FEL (see Methods for details). While complex phase shapes may be implemented with this scheme, for the current objective of controlling the strong-field induced

dynamics in He atoms, shaping the quadratic phase term (group delay dispersion - GDD) is sufficient [44]. Therefore, we focus on the GDD-control in the following discussion.

Figure 3 demonstrates the quantum control of the dressed He populations. The eKE distribution shows a pronounced dependence on the GDD of the XUV pulses (Fig. 3a). At minimum chirp (GDD= 135 fs²), we observe an almost even amplitude in the AT doublet, whereas for GDD < 0 the higher energy photoelectron band dominates and for GDD > 0 the situation is reversed. These changes directly reflect the control of the relative populations in the upper/lower dressed state of the He atoms. We obtain an excellent control contrast and the results are highly robust (Supp. Info. II), which is remarkable given the complex experimental setup. The experiment is in good agreement with the theoretical model (Fig. 3b) numerically solving the time-dependent Schrödinger equation for a single active electron (TDSE-SAE, see Methods for details). To maximize the attainable energy resolution, broadening due to spatial intensity averaging and the instrument response function are not included in the model. This explains the much sharper features in Fig. 3b and the observation of spectral fringes reflecting the temporal progression of the Rabi frequency during the light-matter interaction. The high reproducibility, the excellent control contrast and the good agreement with theory confirm the feasibility of precise pulse shaping in the XUV domain and of quantum control applications, even of transient strong-field phenomena. This marks an important achievement in view of quantum optimal control applications at short wavelengths.

The active control of quantum dynamics with tailored light fields is one asset of pulse shaping. As another asset, systematic studies with shaped laser pulses can be used to unravel underlying physical mechanisms otherwise hidden [49]. Here, we demonstrate this concept for pulse shaping in the XUV domain. The high XUV intensities used in our study lead to a peculiar scenario in which both bound and continuum states are dressed and a complex interplay between their dynamics arises. Hence, for a comprehensive understanding of the strong-field physics taking place, the bound-state dynamics and the non-perturbative photoionization have to be considered. This is in contrast to the strong-field control at long wavelengths, where the continuum could be described perturbatively [44].

Fig. 4a,b show the avoided crossing of the photoelectron bands for different spectral phase curvatures applied to the XUV pulses. The experimental data reveals a clear dependence of the AT doublet amplitudes on the detuning and the GDD of the driving field, in good agreement with theory. In the strong dressing regime, the bound-continuum coupling marks a third factor which influences the photoelectron spectrum. As predicted by theory, this effect leads to an asymmetry in the coupling of the upper/lower dressed state to the continuum [29], which is in agreement with the prevalent asymmetry of the AT doublet amplitudes observed in our data and calculations (Fig. 4a,b). An analogous effect is observed for the strong-field bound-continuum coupling in solid state systems [50].

To disentangle this strong-field effect from the influence

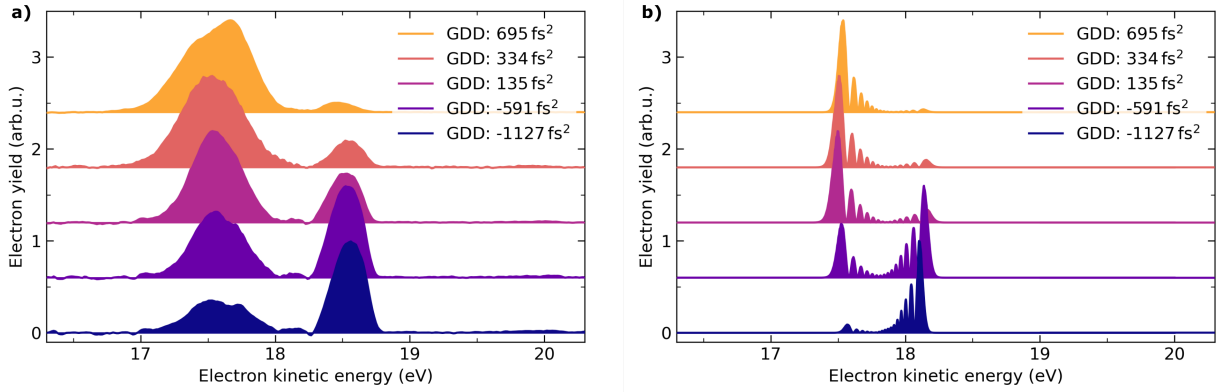


Figure 3. Strong-field quantum control of dressed He populations for the He $1s^2 \rightarrow 1s2p$ resonance (photon energy: 21.25 eV, $I_{\text{eff}} = 2.8(2) \times 10^{14} \text{W/cm}^2$). (a) Photoelectron spectra obtained for phase-shaped XUV pulses (see given GDD values). The control of the dressed state populations is directly reflected in the relative change of amplitude in the photoelectron bands. (b) TDSE-SAE calculations of the light-controlled quantum dynamics. The model underestimates the atomic dipole moment which leads to a slightly smaller AT energy splitting compared to the experimental data. Spectral broadening by the instrument response function and the focal intensity averaging have been omitted in the calculation.

of the detuning and spectral phase of the driving field, we evaluate the amplitude ratio between the upper/lower photoelectron bands at detuning $\delta = 0$ eV (Fig. 4c). Interpolation to $\text{GDD} = 0 \text{fs}^2$ isolates the asymmetry solely caused by the strong-field bound-continuum coupling. We find reasonable agreement with our model when including the dressing of the ionization continuum (blue curve), in stark contrast to the same model but treating the continuum perturbatively (yellow curve). Hence, the dressing of the He atoms provides here a probe of the strong-field dynamics in the continuum. This property is otherwise difficult to access and becomes available by our systematic study of the spectral phase dependence on the photoelectron spectrum.

Another possible mechanism for a general asymmetry in the AT doublet amplitudes could be the interference between ionization pathways via resonant and near-resonant bound states as recently suggested for the dressing of He atoms with XUV [19, 51] and for alkali atoms with bichromatic near infrared fields [52]. For helium such effects are, however, expected in a narrow parameter range [19, 51], which lies outside the regime probed in our experiment. For confirmation, we suppressed the resonant ionization path in our model, which eliminates possible interference effects. Still, we observe a pronounced asymmetry in the AT doublet amplitudes (not shown). We thus assign the experimental observation to the coupling of the dressed atom dynamics with a dressed ionization continuum induced by intense XUV driving fields.

A comprehensive understanding of the strong-field induced dynamics in the system lays the basis for another quantum control effect, that is the suppression of the system's ionization rate, as proposed theoretically [29]. The excitation probability for one-photon transitions is generally independent of the chirp direction of the driving field. However, if driving a quantum system in the strong-field limit, its quasi-resonant two-photon ionization rate may become sensitive to the chirp direction. We demonstrate the effect experimentally in Fig. 4d. A substantial reduction of the He ionization rate by 64% is achieved, solely by tuning the chirp of the FEL pulses while

keeping the pulse area constant. The good agreement with the TDSE-SAE calculations confirms the mechanism. This control scheme exploits the interplay between the bound-state dynamics and the above discussed selective coupling of the upper/lower dressed state to the ionization continuum. We note a stabilization mechanism of the dressed states in He was recently proposed, effectively causing also a suppression of the ionization rate [51]. This mechanism requires, however, extreme pulse parameters, difficult to achieve experimentally. In contrast, our approach based on shaped pulses is more feasible and applies to a broader parameter range.

With this work, we have established a new tool for the manipulation and control of matter using XUV light sources. Both the quantum control of dressed state populations and the disentanglement of bound and continuum dressing was demonstrated with phase-shaped XUV pulses, in good agreement with theoretical predictions. Moreover, chirp control of the FEL pulses enabled a substantial reduction of the system's ionization rate, with prospective implications in many XUV/X-ray spectroscopy and diffraction imaging applications, where typically high radiation intensities are applied and sample ionization marks a major loss channel. We expect our work to stimulate other experimental and theoretical activities exploring the exciting possibilities offered by XUV and X-ray pulse shaping: first theory proposals in this direction have already been made [28–30]. The combination of high laser intensities and pulse shaping could enable population transfer with unit efficiency in rapid adiabatic passage schemes [5, 53]. This may find applications, e.g. in valence-core stimulated Raman scattering [54] or in efficient and fast qubit manipulation with XUV and X-ray light. The recent progress in echo-enabled harmonic generation [55] promises to extend the pulse shaping concept to much higher photon energies where localized core-electron states can be addressed. The generation of coherent attosecond pulse trains, with independent control of amplitude and phases has been demonstrated at seeded FELs [36], bringing pulse shaping applications on the attosecond time scale into reach. This opens an exciting avenue towards the

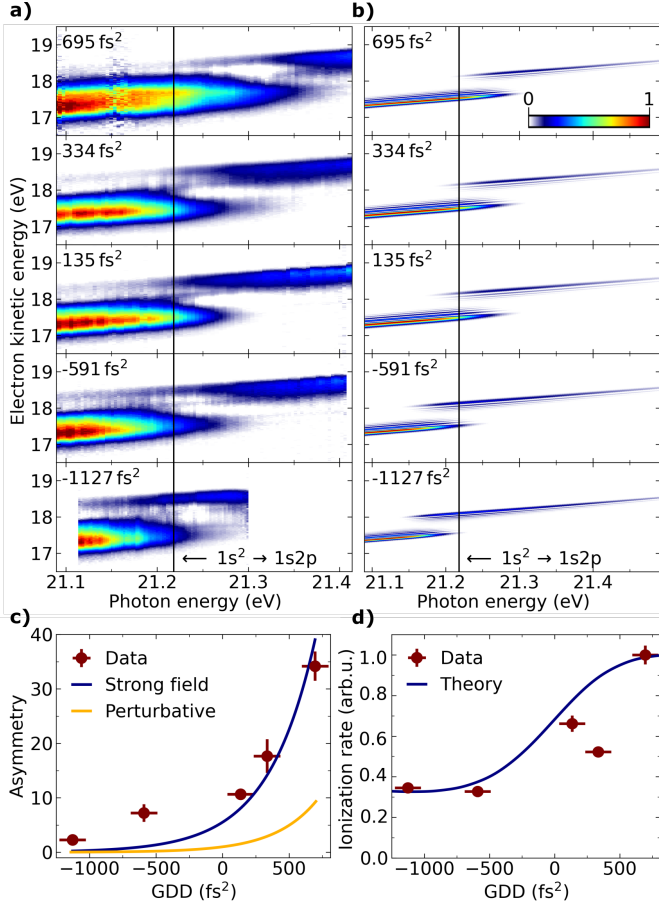


Figure 4. Energy-domain representation of the quantum control scheme. (a) Photoelectron spectra as a function of energy detuning for different GDD values as labeled ($I_{\text{eff}} = 2.92(18) \times 10^{14} \text{ W/cm}^2$). (b) TDSE-SAE calculations. Broadening by the instrument response function is omitted in the model. (c) Amplitude ratio between upper/lower photoelectron bands evaluated at the $1s^2 \rightarrow 1s2p$ resonance, hence $\delta = 0$. Experimental data (red), TDSE-SAE model treating the bound and continuum dynamics non-perturbatively (blue), TDSE-SAE model applied to the bound state dynamics, but treating the continuum perturbatively (yellow). (d) Dependence of the He ionization rate on the spectral phase of the driving field. Data (red), TDSE-SAE model (blue).

quantum control of molecular and solid state systems with chemical selectivity and on attosecond time scales.

III. METHODS

A. Experiment

The experiments were performed at the low density matter (LDM) endstation [56] of the FEL FERMI-1 [48]. The FEL was operated in circular polarization at the 6th harmonic of the seed laser. The FEL photon energy was tuned in the 21.05 eV to 21.47 eV range with an optical parametric amplifier in the seed laser setup. Maximum pulse energy at the target was $E_{\text{max}} = 71 \mu\text{J}$, taking transmission losses into account. A N_2 -gas filter was used for continuous attenuation of the pulse energy. For the data in Fig. 2c, a Sn-filter (thickness: 200 nm) was inserted, attenuating the XUV intensity by roughly one order of magnitude. At minimum chirp setting (GDD = 135 fs²), an FEL pulse duration of 49(3) fs was measured by a cross-correlation between the FEL pulses and an 800-nm auxiliary

pulse. The beam size at the target was $8.00(8) \times 11.3(1) \mu\text{m}^2$, reconstructed with a Hartmann wavefront sensor. Assuming a Gaussian spatial mode, this yields a calculated estimate for the maximum reachable peak intensity of $3.84 \times 10^{14} \text{ W/cm}^2$ at the interaction region. In comparison, the effective intensity deduced from the AT splitting is $I_{\text{eff}} = 2.78(2) \times 10^{14} \text{ W/cm}^2$. This value is 27% smaller than the value calculated for a Gaussian spatial mode, hinting at an aberrated spatial mode (see also Supp. Info. I).

Spectral phase shaping of the seed laser was implemented by tuning a single-pass transmission grating compressor and characterized by self-diffraction frequency-resolved optical gating (SD-FROG). In the applied tuning range, changes of higher-order phase terms are small and are thus neglected. The coherent transfer of the seed phase ϕ_s to the FEL phase ϕ_{nH} was characterized for a set of seed laser and FEL settings prior to the beamtime using a procedure outlined in Ref. [45]. To minimize the additional chirp introduced by the FEL amplification process (ϕ_a), the FEL amplification was kept reasonably low and only five (out of six) undulators were used. At these conditions, ϕ_a is supposed to be negligible. With these precautions and based on the seed laser GDD, we estimate the uncertainty on the GDD of the FEL to be $\pm 100 \text{ fs}^2$.

At the endstation, a pulsed valve was used at room temperature to create a pulsed beam of He atoms synchronized with the arrival of the XUV pulses. In the interaction region, the atomic beam intersected the laser pulses perpendicularly and the generated photoelectrons were detected with a magnetic bottle electron spectrometer (MBES). A retardation potential of 14 eV was applied to optimize the detector resolution. For the FEL settings used, the contribution of second harmonic FEL emission to the ionization yield is expected to be at least three orders of magnitude smaller and can thus be neglected. For the experimental parameters used, space charge effects can be neglected as confirmed by measurements with different atom densities in the ionization volume. A distortion of photoelectron trajectories by the large retardation potentials was ruled out by simulations of the electron trajectories.

B. Theory

In order to calculate the photoelectron spectra we solve the time-dependent Schrödinger equation (TDSE) for a single-active-electron (SAE) model of the He atom. The effective potential in this model reads

$$V(r) = -\frac{1}{r} [1 + e^{-r/r_0} - re^{-r/r_1}], \quad (2)$$

where r denotes the radial coordinate. It has the correct asymptotic behavior for $r \rightarrow 0$ and $r \rightarrow \infty$ and the values of $r_0 = 0.5670 \text{ \AA}$ and $r_1 = 0.4396 \text{ \AA}$ guarantee that the binding energies $E_{1s^2} = -24.5874 \text{ eV}$ and $E_{1s2p} = -3.3694 \text{ eV}$ of He [57] are reproduced. The dipole moment in this model is slightly smaller than the NIST value [57], which is the reason for the smaller AT splitting obtained in calculations compared to the experimental data. Field-free eigenstates up to an angular momentum of $\ell=3$ are calculated in a box of radius $R = 1.69 \times 10^4 \text{ \AA}$ by means of the Numerov method and are

used as a basis for the TDSE, which is solved in the velocity form. The box size R is chosen sufficiently large to omit the need of absorbing boundary conditions. Thus, photoelectron spectra can be calculated directly from the occupations of the field-free eigenstates obtained in the propagation. Due to the high intensities of interest we treat the vector potential of the FEL pulse classically and use a Gaussian envelope.

C. Data analysis

The photoelectron spectra were background-corrected and filtered w.r.t. fluctuations in FEL pulse energy and photon energy. The effective intensity I_{eff} was calibrated from the AT splitting taken at the maximum pulse energy according to

$$I_{\text{eff}} = 0.5\epsilon_0 c \left(\frac{\hbar\Omega}{\mu} \right)^2. \quad (3)$$

To this end the AT splitting $\hbar\Omega$ was deduced by fitting the corresponding photoelectron spectrum with a sum of three Gaussian functions. For all other pulse energies, the prediction by Eq.3 was plotted as dashed lines in Fig.2a. The Rabi period was calculated based on the determined effective FEL intensity.

The low intensity contribution in the data shown in Fig. 3a was removed by fitting the data with a sum of three Gaussians of which only the amplitude was fitted as free parameter. The fitted Gaussian in the center was subtracted from the data. For the data shown in Fig.4a, the low intensity distribution was removed by subtracting the photoelectron spectrum shown in Fig.2c scaled in amplitude to account for the different pulse energies used in the two data sets.

To determine the ratio between the upper and lower photoelectron band shown in Fig.4c, we computed the integral of photoelectron intensity in the upper/lower band for a photon energy of 21.22 eV (at $1s^2 \rightarrow 1s2p$ resonance) and divided the values.

ACKNOWLEDGEMENTS

The following funding is acknowledged: Bundesministerium für Bildung und Forschung (BMBF) *LoKo-FEL* (05K16VFB) and *STAR* (05K19VF3), European Research Council (ERC) Starting Grant *MULTIPLEX* (101078689), Deutsche Forschungsgemeinschaft (DFG) RTG 2717 and grant 429805582 (project SA 3470/4-1), Baden-Württemberg Stiftung Eliteprogram for Postdocs, Swedish Research Council and Knut and Alice Wallenberg Foundation, Sweden, Danish Agency for Science, Technology, and Innovation for funding through the instrument center DanScatt.

AUTHOR CONTRIBUTIONS

L.B. conceived the experiment with input from U.S. and M.W.. E.A., M.D., A.D., I.N., F.P. and P.S. implemented and characterized the spectral phase shaping of the FEL. E.A., A.B., L.G., Mi.M., G.P., A.S., M.T. and M.Z. optimized the machine and the laser beam parameters. C.C, M.D.F. and O.P. managed the end-station. F.R., B.A., G.C., K.D., S.D.G., N.G., S.H., F.L., Y.L., C.M., Mo.M., A.M., Ma.M., A.N., N.P.,

K.C.P., N.R., F.S., D.U., B.W., C.C, M.D.F., O.P. and L.B. performed the experiment with input from U.S., M.W., R.F., B.v.I., T.L., G.S. and R.J.S.. F.R. analyzed the data under the supervision of L.B.. U.S. provided the theoretical calculations. L.B. wrote the manuscript with input from all authors.

DISCLOSURES

The authors declare no conflicts of interest.

DATA AVAILABILITY

The data that support the findings of the study are openly available.

CODE AVAILABILITY

The code that supports the findings of the study is available from the corresponding authors on reasonable request.

REFERENCES

- ¹T. Brabec and F. Krausz, “Intense few-cycle laser fields: frontiers of nonlinear optics”, *Rev. Mod. Phys.* **72**, 545–591 (2000).
- ²R. J. Levis, G. M. Menkir, and H. Rabitz, “Selective bond dissociation and rearrangement with optimally tailored, strong-field laser pulses”, *Science* **292**, 709–713 (2001).
- ³B. J. Sussman, D. Townsend, M. Y. Ivanov, and A. Stolow, “Dynamic stark control of photochemical processes”, *Science* **314**, 278–281 (2006).
- ⁴I. I. Rabi, “Space quantization in a gyrating magnetic field”, *Phys. Rev.* **51**, 652–654 (1937).
- ⁵N. V. Vitanov, T. Halfmann, B. W. Shore, and K. Bergmann, “Laser-induced population transfer by adiabatic passage techniques”, *Annu. Rev. Phys. Chem.* **52**, 763–809 (2001).
- ⁶C. Pellegrini, A. Marinelli, and S. Reiche, “The physics of X-ray free-electron lasers”, *Rev. Mod. Phys.* **88**, 015006 (2016).
- ⁷I. Orfanos, I. Makos, I. Lontos, E. Skantzakis, B. Major, A. Nayak, M. Dumergue, S. Kühn, S. Kahaly, K. Varju, G. Sansone, B. Witzel, C. Kalpouzos, L. A. A. Nikolopoulos, P. Tzallas, and D. Charalambidis, “Non-linear processes in the extreme ultraviolet”, *J. Phys. Photonics* **2**, 042003 (2020).
- ⁸L. Young, E. P. Kanter, B. Krässig, Y. Li, A. M. March, S. T. Pratt, R. Santra, S. H. Southworth, N. Rohringer, L. F. DiMauro, G. Doumy, C. A. Roedig, N. Berrah, L. Fang, M. Hoener, P. H. Bucksbaum, J. P. Cryan, S. Ghimire, J. M. Glowia, D. A. Reis, J. D. Bozek, C. Bostedt, and M. Messerschmidt, “Femtosecond electronic response of atoms to ultra-intense X-rays”, *Nature* **466**, 56–61 (2010).
- ⁹E. P. Kanter, B. Krässig, Y. Li, A. M. March, P. Ho, N. Rohringer, R. Santra, S. H. Southworth, L. F. DiMauro, G. Doumy, C. A. Roedig, N. Berrah, L. Fang, M. Hoener, P. H. Bucksbaum, S. Ghimire, D. A. Reis, J. D. Bozek, C. Bostedt, M. Messerschmidt, and L. Young, “Unveiling and driving hidden resonances with high-fluence, high-intensity X-ray pulses”, *Phys. Rev. Lett.* **107**, 233001 (2011).

- ¹⁰C. Ott, A. Kaldun, L. Argenti, P. Raith, K. Meyer, M. Laux, Y. Zhang, A. Blättermann, S. Hagstotz, T. Ding, R. Heck, J. Madroñero, F. Martín, and T. Pfeifer, “Reconstruction and control of a time-dependent two-electron wave packet”, *Nature* **516**, 374–378 (2014).
- ¹¹T. E. Glover, M. P. Hertlein, S. H. Southworth, T. K. Allison, J. van Tilborg, E. P. Kanter, B. Krässig, H. R. Varma, B. Rude, R. Santra, A. Belkacem, and L. Young, “Controlling X-rays with light”, *Nat. Phys.* **6**, 69–74 (2010).
- ¹²P. Ranitovic, X. M. Tong, C. W. Hogle, X. Zhou, Y. Liu, N. Toshima, M. M. Murnane, and H. C. Kapteyn, “Controlling the XUV transparency of helium using two-pathway quantum interference”, *Phys. Rev. Lett.* **106**, 193008 (2011).
- ¹³M. Fushitani, C.-N. Liu, A. Matsuda, T. Endo, Y. Toida, M. Nagasono, T. Togashi, M. Yabashi, T. Ishikawa, Y. Hikosaka, T. Morishita, and A. Hishikawa, “Femtosecond two-photon Rabi oscillations in excited He driven by ultrashort intense laser fields”, *Nat. Photonics* **10**, 102–105 (2016).
- ¹⁴C. Ott, L. Aufleger, T. Ding, M. Rebholz, A. Magunia, M. Hartmann, V. Stooß, D. Wachs, P. Birk, G. D. Borisova, K. Meyer, P. Rupprecht, C. da Costa Castanheira, R. Moshhammer, A. R. Attar, T. Gaumnitz, Z.-H. Loh, S. Düsterer, R. Treusch, J. Ullrich, Y. Jiang, M. Meyer, P. Lambropoulos, and T. Pfeifer, “Strong-field extreme-ultraviolet dressing of atomic double excitation”, *Phys. Rev. Lett.* **123**, 163201 (2019).
- ¹⁵M. Meyer, D. Cubaynes, V. Richardson, J. T. Costello, P. Radcliffe, W. B. Li, S. Düsterer, S. Fritzsche, A. Mihelic, K. G. Papamihail, and P. Lambropoulos, “Two-photon excitation and relaxation of the 3d-4d resonance in atomic Kr”, *Phys. Rev. Lett.* **104**, 213001 (2010).
- ¹⁶T. Sako, J. Adachi, A. Yagishita, M. Yabashi, T. Tanaka, M. Nagasono, and T. Ishikawa, “Suppression of ionization probability due to Rabi oscillations in the resonance two-photon ionization of He by EUV free-electron lasers”, *Phys. Rev. A* **84**, 053419 (2011).
- ¹⁷M. Flögel, J. Durá, B. Schütte, M. Ivanov, A. Rouzée, and M. J. J. Vrakking, “Rabi oscillations in extreme ultraviolet ionization of atomic argon”, *Phys. Rev. A* **95**, 021401 (2017).
- ¹⁸T. Ding, M. Rebholz, L. Aufleger, M. Hartmann, K. Meyer, V. Stooß, A. Magunia, D. Wachs, P. Birk, Y. Mi, G. D. Borisova, C. d. C. Castanheira, P. Rupprecht, Z.-H. Loh, A. R. Attar, T. Gaumnitz, S. Roling, M. Butz, H. Zacharias, S. Düsterer, R. Treusch, S. M. Cavaletto, C. Ott, and T. Pfeifer, “Nonlinear coherence effects in transient-absorption ion spectroscopy with stochastic extreme-ultraviolet free-electron laser pulses”, *Phys. Rev. Lett.* **123**, 103001 (2019).
- ¹⁹S. Nandi, E. Olofsson, M. Bertolino, S. Carlström, F. Zapata, D. Busto, C. Callegari, M. Di Fraia, P. Eng-Johnsson, R. Feifel, G. Gallician, M. Gisselbrecht, S. Maclot, L. Neoričić, J. Peschel, O. Plekan, K. C. Prince, R. J. Squibb, S. Zhong, P. V. Demekhin, M. Meyer, C. Miron, L. Badano, M. B. Danailov, L. Giannessi, M. Manfredda, F. Sottocorona, M. Zangrando, and J. M. Dahlström, “Observation of Rabi dynamics with a short-wavelength free-electron laser”, *Nature* **608**, 488–493 (2022).
- ²⁰M. Z. Stuart A. Rice, *Optical control of molecular dynamics* (Wiley-Interscience, 2000).
- ²¹D. Tannor, *Introduction to quantum mechanics: a time-dependent perspective* (Palgrave Macmillan, Jan. 31, 2007), 662 pp.
- ²²M. Shapiro and P. Brumer, *Quantum control of molecular processes* (John Wiley & Sons, Jan. 18, 2012), 565 pp.
- ²³C. Brif, R. Chakrabarti, and H. Rabitz, “Control of quantum phenomena: past, present and future”, *New J. Phys.* **12**, 075008 (2010).
- ²⁴T. Brixner and G. Gerber, “Quantum control of gas-phase and liquid-phase femtochemistry”, *ChemPhysChem* **4**, 418–438 (2003).
- ²⁵M. Dantus and V. V. Lozovoy, “Experimental coherent laser control of physicochemical processes”, *Chem. Rev.* **104**, 1813–1860 (2004).
- ²⁶M. Wollenhaupt, V. Engel, and T. Baumert, “Femtosecond laser photoelectron spectroscopy on atoms and small molecules: prototype studies in quantum control”, *Annu. Rev. Phys. Chem.* **56**, 25–56 (2005).
- ²⁷T. Pfeifer, R. Spitzenpfeil, D. Walter, C. Winterfeldt, F. Dimler, G. Gerber, and C. Spielmann, “Towards optimal control with shaped soft-x-ray light”, *Opt. Express* **15**, 3409–3416 (2007).
- ²⁸L. Greenman, C. P. Koch, and K. B. Whaley, “Laser pulses for coherent XUV Raman excitation”, *Phys. Rev. A* **92**, 013407 (2015).
- ²⁹U. Saalman, S. K. Giri, and J. M. Rost, “Adiabatic passage to the continuum: controlling ionization with chirped laser pulses”, *Phys. Rev. Lett.* **121**, 153203 (2018).
- ³⁰D. Keefer and S. Mukamel, “Selective enhancement of spectroscopic features by quantum optimal control”, *Phys. Rev. Lett.* **126**, 163202 (2021).
- ³¹K. C. Prince, E. Allaria, C. Callegari, R. Cucini, G. D. Ninno, S. D. Mitri, B. Diviacco, E. Ferrari, P. Finetti, D. Gauthier, L. Giannessi, N. Mahne, G. Penco, O. Plekan, L. Raimondi, P. Rebernik, E. Roussel, C. Svetina, M. Trovò, M. Zangrando, M. Negro, P. Carpeggiani, M. Reduzzi, G. Sansone, A. N. Grum-Grzhimailo, E. V. Gryzlova, S. I. Strakhova, K. Bartschat, N. Douguet, J. Venzke, D. Iablonskyi, Y. Kumagai, T. Takanashi, K. Ueda, A. Fischer, M. Coreno, F. Stienkemeier, Y. Ovcharenko, T. Mazza, and M. Meyer, “Coherent control with a short-wavelength free-electron laser”, *Nat. Photonics* **10**, 176–179 (2016).
- ³²S. Usenko, A. Przystawik, M. A. Jakob, L. L. Lazzarino, G. Brenner, S. Toleikis, C. Haunhorst, D. Kip, and T. Laarmann, “Attosecond interferometry with self-amplified spontaneous emission of a free-electron laser”, *Nat. Commun* **8**, 15626 (2017).
- ³³A. Wituschek, L. Bruder, E. Allaria, U. Bangert, M. Binz, R. Borghes, C. Callegari, G. Cerullo, P. Cinquegrana, L. Giannessi, M. Danailov, A. Demidovich, M. D. Fraia, M. Drabbels, R. Feifel, T. Laarmann, R. Michiels, N. S. Mirian, M. Mudrich, I. Nikolov, F. H. O’Shea, G. Penco, P. Piseri, O. Plekan, K. C. Prince, A. Przystawik, P. R. Ribič, G. Sansone, P. Sigalotti, S. Spampinati, C. Spezzani, R. J. Squibb, S. Stranges, D. Uhl, and F. Stienkemeier, “Tracking attosecond electronic coherences using phase-manipulated extreme ultraviolet pulses”, *Nat. Commun* **11**, 883 (2020).

- ³⁴K. P. Heeg, A. Kaldun, C. Strohm, C. Ott, R. Subramanian, D. Lentrodt, J. Haber, H.-C. Wille, S. Goerttler, R. Ruffer, C. H. Keitel, R. Röhlsberger, T. Pfeifer, and J. Evers, “Coherent X-ray-optical control of nuclear excitons”, *Nature* **590**, 401–404 (2021).
- ³⁵L.-M. Koll, L. Maikowski, L. Drescher, T. Witting, and M. J. J. Vrakking, “Experimental control of quantum-mechanical entanglement in an attosecond pump-probe experiment”, *Phys. Rev. Lett.* **128**, 043201 (2022).
- ³⁶P. K. Maraju, C. Grazioli, M. D. Fraia, M. Moiola, D. Ertel, H. Ahmadi, O. Plekan, P. Finetti, E. Allaria, L. Giannessi, G. D. Ninno, C. Spezzani, G. Penco, S. Spampinati, A. Demidovich, M. B. Danailov, R. Borghes, G. Kourousias, C. E. S. D. Reis, F. Billé, A. A. Lutman, R. J. Squibb, R. Feifel, P. Carpeggiani, M. Reduzzi, T. Mazza, M. Meyer, S. Bengtsson, N. Ibrakovic, E. R. Simpson, J. Mauritsson, T. Csizmadia, M. Dumergue, S. Kühn, H. N. Gopalakrishna, D. You, K. Ueda, M. Labeye, J. E. Bækhoj, K. J. Schafer, E. V. Gryzlova, A. N. Grum-Grzhimailo, K. C. Prince, C. Callegari, and G. Sansone, “Attosecond pulse shaping using a seeded free-electron laser”, *Nature* **578**, 386–391 (2020).
- ³⁷P. K. Maraju, M. Di Fraia, O. Plekan, M. Bonanomi, B. Merzuk, D. Busto, I. Makos, M. Schmoll, R. Shah, P. R. Ribič, L. Giannessi, G. De Ninno, C. Spezzani, G. Penco, A. Demidovich, M. Danailov, M. Coreno, M. Zangrando, A. Simoncig, M. Manfredda, R. J. Squibb, R. Feifel, S. Bengtsson, E. R. Simpson, T. Csizmadia, M. Dumergue, S. Kühn, K. Ueda, J. Li, K. J. Schafer, F. Frassetto, L. Poletto, K. C. Prince, J. Mauritsson, C. Callegari, and G. Sansone, “Attosecond coherent control of electronic wave packets in two-colour photoionization using a novel timing tool for seeded free-electron laser”, *Nat. Photonics* **17**, 200–207 (2023).
- ³⁸G. Perosa, J. Wätzel, D. Garzella, E. Allaria, M. Bonanomi, M. B. Danailov, A. Brynes, C. Callegari, G. De Ninno, A. Demidovich, M. Di Fraia, S. Di Mitri, L. Giannessi, M. Manfredda, L. Novinec, N. Pal, G. Penco, O. Plekan, K. C. Prince, A. Simoncig, S. Spampinati, C. Spezzani, M. Zangrando, J. Berakdar, R. Feifel, R. J. Squibb, R. Coffee, E. Hemsing, E. Roussel, G. Sansone, B. W. J. McNeil, and P. R. Ribič, “Femtosecond polarization shaping of free-electron laser pulses”, *Phys. Rev. Lett.* **131**, 045001 (2023).
- ³⁹C. Cohen-Tannoudji, J. Dupont-Roc, and G. Grynberg, *Atom-photon interactions: basic processes and applications* (John Wiley & Sons, Mar. 23, 1998), 691 pp.
- ⁴⁰S. H. Autler and C. H. Townes, “Stark effect in rapidly varying fields”, *Phys. Rev.* **100**, 703–722 (1955).
- ⁴¹M. Wollenhaupt, A. Präkelt, C. Sarpe-Tudoran, D. Liese, T. Bayer, and T. Baumert, “Femtosecond strong-field quantum control with sinusoidally phase-modulated pulses”, *Phys. Rev. A* **73**, 063409 (2006).
- ⁴²T. Jahnke, U. Hergenhahn, B. Winter, R. Dörner, U. Fröhling, P. V. Demekhin, K. Gokhberg, L. S. Cederbaum, A. Ehresmann, A. Knie, and A. Dreuw, “Interatomic and intermolecular coulombic decay”, *Chem. Rev.* **120**, 11295–11369 (2020).
- ⁴³T. Bayer, M. Wollenhaupt, H. Braun, and T. Baumert, “Ultrafast and efficient control of coherent electron dynamics via SPODS”, in *Advances in chemical physics* (John Wiley & Sons, Ltd, 2016) Chap. 6, pp. 235–282.
- ⁴⁴M. Wollenhaupt, A. Präkelt, C. Sarpe-Tudoran, D. Liese, and T. Baumert, “Quantum control by selective population of dressed states using intense chirped femtosecond laser pulses”, *Appl. Phys. B* **82**, 183–188 (2006).
- ⁴⁵D. Gauthier, P. R. Ribič, G. De Ninno, E. Allaria, P. Cinquegrana, M. B. Danailov, A. Demidovich, E. Ferrari, L. Giannessi, B. Mahieu, and G. Penco, “Spectrotemporal shaping of seeded free-electron laser pulses”, *Phys. Rev. Lett.* **115**, 114801 (2015).
- ⁴⁶G. De Ninno, D. Gauthier, B. Mahieu, P. R. Ribič, E. Allaria, P. Cinquegrana, M. B. Danailov, A. Demidovich, E. Ferrari, L. Giannessi, G. Penco, P. Sigalotti, and M. Stupar, “Single-shot spectro-temporal characterization of XUV pulses from a seeded free-electron laser”, *Nat. Commun* **6**, 8075 (2015).
- ⁴⁷D. Gauthier, E. Allaria, M. Coreno, I. Cudin, H. Dacasa, M. B. Danailov, A. Demidovich, S. Di Mitri, B. Diviacco, E. Ferrari, P. Finetti, F. Frassetto, D. Garzella, S. Künzel, V. Leroux, B. Mahieu, N. Mahne, M. Meyer, T. Mazza, P. Miotti, G. Penco, L. Raimondi, P. R. Ribič, R. Richter, E. Roussel, S. Schulz, L. Sturari, C. Svetina, M. Trovò, P. A. Walker, M. Zangrando, C. Callegari, M. Fajardo, L. Poletto, P. Zeitoun, L. Giannessi, and G. De Ninno, “Chirped pulse amplification in an extreme-ultraviolet free-electron laser”, *Nat. Commun* **7**, 13688 (2016).
- ⁴⁸E. Allaria, R. Appio, L. Badano, W. A. Barletta, S. Basanese, S. G. Biedron, A. Borga, E. Busetto, D. Castronovo, P. Cinquegrana, S. Cleva, D. Cocco, M. Cornacchia, P. Craievich, I. Cudin, G. D’Auria, M. Dal Forno, M. B. Danailov, R. De Monte, G. De Ninno, P. Delgiusto, A. Demidovich, S. Di Mitri, B. Diviacco, A. Fabris, R. Fabris, W. Fawley, M. Ferianis, E. Ferrari, S. Ferry, L. Froehlich, P. Furlan, G. Gaio, F. Gelmetti, L. Giannessi, M. Giannini, R. Gobessi, R. Ivanov, E. Karantzoulis, M. Lonza, A. Lutman, B. Mahieu, M. Milloch, S. V. Milton, M. Musardo, I. Nikolov, S. Noe, F. Parmigiani, G. Penco, M. Petronio, L. Pivetta, M. Predonzani, F. Rossi, L. Rumiz, A. Salom, C. Scafuri, C. Serpico, P. Sigalotti, S. Spampinati, C. Spezzani, M. Svandrlik, C. Svetina, S. Tazzari, M. Trovo, R. Umer, A. Vascotto, M. Veronese, R. Visintini, M. Zaccaria, D. Zangrando, and M. Zangrando, “Highly coherent and stable pulses from the FERMI seeded free-electron laser in the extreme ultraviolet”, *Nat. Photonics* **6**, 699–704 (2012).
- ⁴⁹C. J. Bardeen, Q. Wang, and C. V. Shank, “Selective excitation of vibrational wave packet motion using chirped pulses”, *Phys. Rev. Lett.* **75**, 3410–3413 (1995).
- ⁵⁰F. Mahmood, C.-K. Chan, Z. Alpichshev, D. Gardner, Y. Lee, P. A. Lee, and N. Gedik, “Selective scattering between Floquet–Bloch and Volkov states in a topological insulator”, *Nat. Phys.* **12**, 306–310 (2016).
- ⁵¹E. Olofsson and J. M. Dahlström, “Photoelectron signature of dressed-atom stabilization in an intense XUV field”, *Phys. Rev. Res.* **5**, 043017 (2023).
- ⁵²T. Bayer, K. Eickhoff, D. Köhnke, and M. Wollenhaupt, “Bichromatic phase-control of interfering Autler-Townes spectra”, 10.48550/arXiv.2311.08248 (2024).

- ⁵³K. Bergmann, H. Theuer, and B. W. Shore, “Coherent population transfer among quantum states of atoms and molecules”, *Rev. Mod. Phys.* **70**, 1003–1025 (1998).
- ⁵⁴J. T. O’Neal, E. G. Champenois, S. Oberli, R. Obaid, A. Al-Haddad, J. Barnard, N. Berrah, R. Coffee, J. Duris, G. Galinis, D. Garratt, J. M. Glowina, D. Haxton, P. Ho, S. Li, X. Li, J. MacArthur, J. P. Marangos, A. Natan, N. Shivaram, D. S. Slaughter, P. Walter, S. Wandel, L. Young, C. Bostedt, P. H. Bucksbaum, A. Picón, A. Marinelli, and J. P. Cryan, “Electronic population transfer via impulsive stimulated X-ray Raman scattering with attosecond soft-x-ray pulses”, *Phys. Rev. Lett.* **125**, 073203 (2020).
- ⁵⁵P. Rebernik Ribič, A. Abrami, L. Badano, M. Bossi, H.-H. Braun, N. Bruchon, F. Capotondi, D. Castronovo, M. Cautero, P. Cinquegrana, M. Coreno, M. E. Couprie, I. Cudin, M. Boyanov Danailov, G. De Ninno, A. Demidovich, S. Di Mitri, B. Diviacco, W. M. Fawley, C. Feng, M. Feriannis, E. Ferrari, L. Foglia, F. Frassetto, G. Gaio, D. Garzella, A. Ghaith, F. Giacuzzo, L. Giannessi, V. Grattoni, S. Grulja, E. Hemsing, F. Iazzourene, G. Kurdi, M. Lonza, N. Mahne, M. Malvestuto, M. Manfredda, C. Masciovecchio, P. Miotti, N. S. Mirian, I. Petrov Nikolov, G. M. Penco, G. Penn, L. Poletto, M. Pop, E. Prat, E. Principi, L. Raimondi, S. Reiche, E. Roussel, R. Sauro, C. Scafuri, P. Sigalotti, S. Spampinati, C. Spezzani, L. Sturari, M. Svandrlik, T. Tanikawa, M. Trovó, M. Veronese, D. Vivoda, D. Xiang, M. Zaccaria, D. Zangrando, M. Zangrando, and E. M. Allaria, “Coherent soft X-ray pulses from an echo-enabled harmonic generation free-electron laser”, *Nat. Photonics* **13**, 555–561 (2019).
- ⁵⁶V. Lyamayev, Y. Ovcharenko, R. Katzy, M. Devetta, L. Bruder, A. LaForge, Marcel Mudrich, U. Person, F. Stienkemeier, M. Krikunova, T. Möller, P. Piseri, Lorenzo Avaldi, M. Coreno, P. O’Keeffe, P. Bolognesi, M. Alagia, A. Kivimäki, M. D. Fraia, N. B. Brauer, M. Drabbels, T. Mazza, S. Stranges, P. Finetti, Cesare Grazioli, O. Plekan, R. Richter, K. C. Prince, and C. Callegari, “A modular end-station for atomic, molecular, and cluster science at the low density matter beamline of FERMI@Elettra”, *J. Phys. B: At. Mol. Opt. Phys.* **46**, 164007 (2013).
- ⁵⁷Kramida, A., Ralchenko, Yu., Reader, J., and NIST ASD Team, *NIST atomic spectra database (ver. 5.3)*, National Institute of Standards and Technology, Gaithersburg, MD, (July 21, 2015) <http://physics.nist.gov/asd> (visited on 07/21/2015).

Supplementary Information: Strong-field quantum control by pulse shaping in the extreme ultraviolet domain

Fabian Richter¹, Ulf Saalman², Enrico Allaria³, Matthias Wollenhaupt⁴, Benedetto Ardingi⁵, Alexander Brynes³, Carlo Callegari³, Giulio Cerullo⁵, Miltcho Danailov³, Alexander Demidovich³, Katrin Dulitz⁶, Raimund Feifel⁷, Michele Di Fraia^{3,8}, Sarang Dev Ganeshamandiram¹, Luca Giannessi^{3,9}, Nicolai Gözl¹, Sebastian Hartweg¹, Bernd von Issendorff¹, Tim Laarmann^{10,11}, Friedemann Landmesser¹, Yilin Li¹, Michele Manfreda³, Cristian Manzoni¹², Moritz Michelbach¹, Arne Morlok¹, Marcel Mudrich¹³, Aaron Ngai¹, Ivaylo Nikolov³, Nitish Pal³, Fabian Pannek¹⁴, Giuseppe Penco³, Oksana Plekan³, Kevin C. Prince³, Giuseppe Sansone¹, Alberto Simoncig³, Frank Stienkemeier¹, Richard James Squibb⁷, Peter Susnjar³, Mauro Trovo³, Daniel Uhl¹, Brendan Wouterlood¹, Marco Zangrando^{3,8}, Lukas Bruder^{1,*}

¹Institute of Physics, University of Freiburg, Hermann-Herder-Str. 3, D-79104 Freiburg, Germany

²Max-Planck-Institut für Physik komplexer Systeme, Nöthnitzer Str. 38, 01187 Dresden, Germany

³Elettra-Sincrotrone Trieste S.C.p.A., 34149 Basovizza (Trieste), Italy

⁴Institute of Physics, University of Oldenburg, Carl-von-Ossietzky-Str. 9-11, 26129 Oldenburg, Germany

⁵IFN-CNR, Dipartimento di Fisica, Piazza L. Da Vinci 32, 20133 Milan, Italy

⁶Institut für Ionenphysik und Angewandte Physik, Universität Innsbruck, 6020 Innsbruck, Austria

⁷Department of Physics, University of Gothenburg, Origovägen 6 B, SE-412 96 Gothenburg, Sweden

⁸Istituto Officina dei Materiali - CNR (CNR-IOM), Strada Statale 14 – km 163.5, Trieste, 34149, Italy

⁹Istituto Nazionale di Fisica Nucleare - Laboratori Nazionali di Frascati, Via E. Fermi 40, 00044

Frascati, Roma

¹⁰Deutsches Elektronen-Synchrotron DESY, Notkestr. 85, 22607 Hamburg, Germany

¹¹The Hamburg Centre for Ultrafast Imaging CUI, Luruper Chaussee 149, 22761 Hamburg, Germany

¹²IFN-CNR, Piazza L. Da Vinci 32, 20133 Milan, Italy

¹³Department of Physics and Astronomy, Aarhus University, Ny Munkegade 120, DK-8000 Aarhus,

Denmark

¹⁴Institute for Experimental Physics, University of Hamburg, Luruper Chaussee 149, 22761 Hamburg,

Germany

I. SPATIAL INTENSITY DISTRIBUTION IN THE INTERACTION VOLUME

The spatial intensity distribution in the ionization volume of the experiment was measured with a Hartmann wavefront sensor. The atomic jet target has a width of ≈ 0.2 mm along the FEL propagation direction, thus the intensity in the direction of propagation can be assumed to be constant. To visualize the intensity distribution in the transverse mode, we generated a histogram of the intensity values measured in the ionization volume (Fig. 1). The experimental distribution (blue) is compared to an ideal Gaussian TEM_{00} mode (orange). While the TEM_{00} mode is characterized by an equal relative occurrence of all intensity values in the ionization volume, the actual intensity occurrences measured in the experiment show a maximum at intensities roughly three orders of magnitude lower than the peak intensity I_0 . Hence, in the experiment a much larger fraction of He atoms in the ionization volume were excited by low intensities than expected theoretically. At these low intensities, the AT splitting is too small to be resolved. This rationalizes the appearance of a pronounced peak in the center of the measured photoelectron spectra not showing an AT splitting.

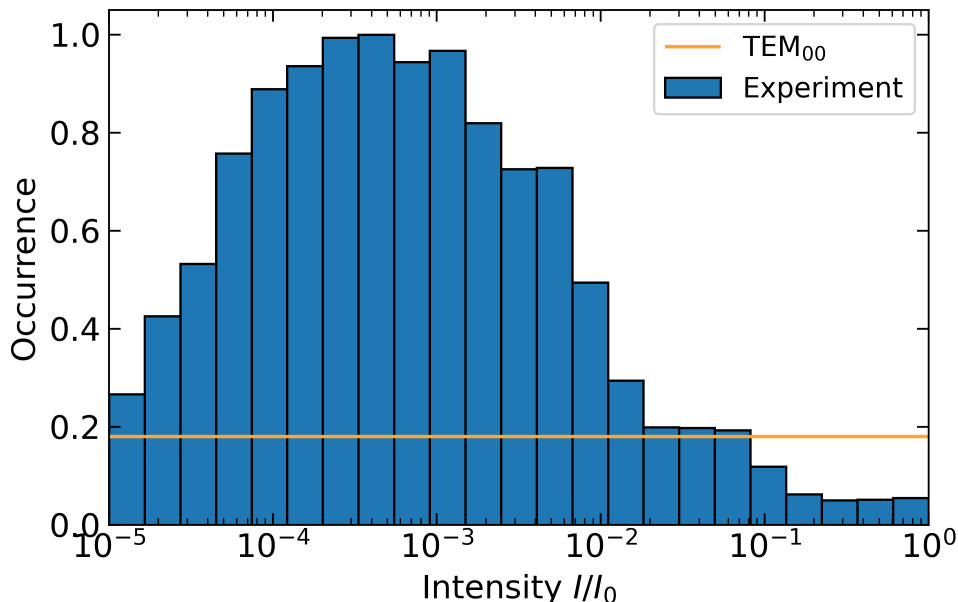


Figure 1. Histogram of the intensities in the ionization volume. Blue: measured distribution, orange: theoretical distribution for TEM_{00} mode. Intensities are given relative to the peak intensity I_0 .

II. REPRODUCIBILITY

Fig. 2 shows examples of raw photoelectron spectra for $\text{GDD} = 135 \text{ fs}^2$ taken before and after acquiring the data shown in Fig. 3a of the main text. Very good agreement between the two spectra is found, even though the chirp settings of the seed laser and thus of the FEL were changed in the range -1127 fs^2 to $+695 \text{ fs}^2$ over the course

*lukas.bruder@physik.uni-freiburg.de

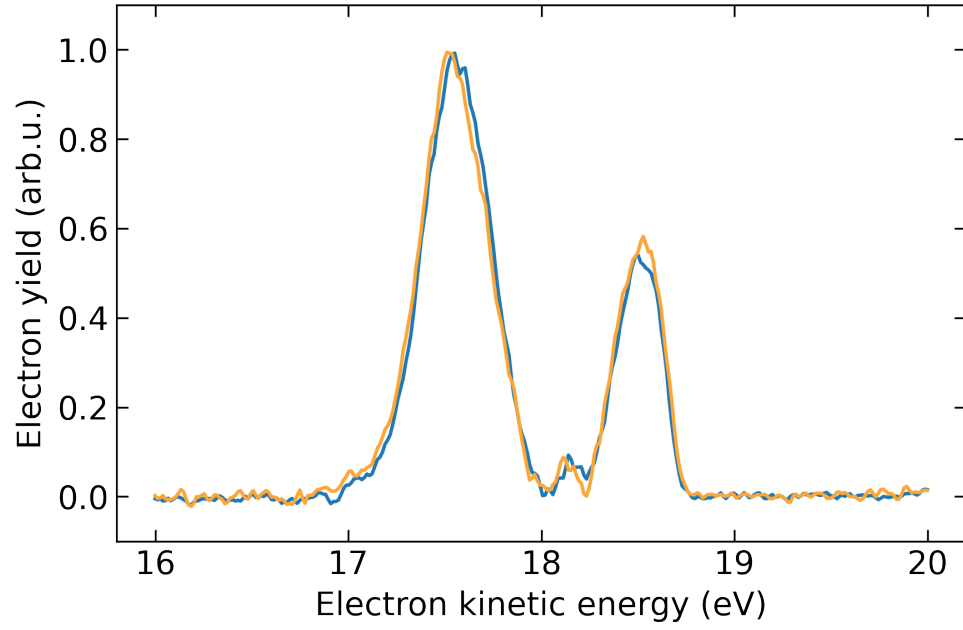


Figure 2. Photoelectron spectra for $\text{GDD}=135 \text{ fs}^2$ of the XUV pulses. The low intensity contribution has been subtracted as done for Fig. 3a in the main text. Orange/blue was taken before/after acquiring the data set in Fig. 3a (main text).

of several hours between the two measurements. This shows the high reproducibility of the XUV pulse shaping method implemented here.